16th East Asia-Pacific Conference on Structural Engineering & Construction (EASEC16)
Edited by C.M. Wang, V. Dao and S. Kitipornchai
Brisbane, Australia, December 3-6, 2019

INVESTIGATIONS INTO COMPRESSION BEHAVIOUR OF T-JOINTS BETWEEN S690 CIRCULAR HOLLOW SECTIONS UNDER BRACE AXIAL FORCE

Y.F. HU[1,2] and K.F. CHUNG[1,2]*

[1]Chinese National Engineering Research Centre for Steel Construction (Hong Kong Branch),
The Hong Kong Polytechnic University, Hong Kong SAR
[2]Department of Civil and Environmental Engineering,
The Hong Kong Polytechnic University, Hong Kong SAR
Emails: yi-fei.hu@polyu.edu.hk, kwok-fai.chung@polyu.edu.hk
*Corresponding author

Abstract. *This paper presents an experimental and numerical investigation into the compression behaviour of T-joints between S690 cold-formed circular hollow sections (CFCHS). A total of four T-joints between S690 CFCHS were tested under axial compression in brace members. A typical failure mode was observed that all joints failed in an interaction between the local plastification of the chords and overall plastic bending of the chords. Three dimensional finite element models with geometrical and material non-linearity have been established and verified after calibration against test results. Both measured geometrical dimensions and material properties of these CFCHS are incorporated into the proposed models. Both the experimental and the numerical results are compared with design resistances obtained from existing design codes, including EN 1993-1-8 and CIDECT Design Guide 1. The investigation will facilitate development of efficient design rules for resistances of T-joints between S690 CFCHS under brace axial compression.*

Keywords: *High strength steel; T-joints; Circular hollow sections; Axial compression.*

1. INTRODUCTION

Structural behaviour of tubular joints between normal strength steel hollow sections have been extensively investigated in the past decades. The research findings have been developed into various design rules adopted by some international design specifications for application. Design recommendations for these tubular joints were proposed by the International Institute of Welding (IIW) Subcommission XV-E in 1981 and 1991(IIW 1981 and 1991). Eurocode EN 1993-1-8 (CEN 2005) adopted the design recommendations proposed by the 2nd edition of IIW recommendations (IIW 1989). The latest version of CIDECT Design Guide 1 (Wardenier et. al. 2008) follows the 3rd editions of IIW recommendations (IIW 2009). Current design rules for high strength steel tubular joints were developed based on extensive numerical results and re-assessment of existing experimental results (Qian et al. 2008). Since there were insufficient experimental results for high strength steel tubular joints available at that time, both strength reduction factors and limitations on the tensile to yield strength ratio, f_u / f_y, were set to ensure a safety margin for practical design. In recent years, there has been an increasing number of research on high strength steel tubular joints. Various joint types with different cross-section geometry were studied to enrich the database on high strength steel tubular joints, for re-

evaluating the current design rules. As many current design rules for high strength CHS T-joints are developed based on the test results on normal strength steel CHS T-joints and extensive numerical analyses results, it is necessary to carry out structural tests on high strength CHS T-joints under brace axial compression to enrich the existing database.

It is also highly desirable to develop finite element models with a high precision to analyze suitability of existing reduction factors on high strength steel CHS T-joints to see whether the design could be improved. Effects of cold-forming, weld-induced residual stresses and strength reduction in heat affected zones on the structural behaviour of these high strength tubular joints are necessary to be further investigated.

2. EXPERIMENTAL INVESTIGATION

2.1. Test programme

In order to investigate the structural behaviour of these high strength S690 welded steel T-joints, a total of four T-joints between cold-formed circular hollow sections (CFCHS) were fabricated and tested under axial compression in brace members. The test programme is presented in Table 1 while Figure 1 presents detailed configuration of a T-joint. The lengths of both the chords and the braces of the joints, L_0 and L_1 are 1200 mm and 600 mm respectively. The span between two pinned supports, L, is 1500 mm.

Table 1. Test programme

Test specimen	Steel grade	Chord member $d_0 \times t_0$ (mm×mm)	Brace member $d_1 \times t_1$ (mm×mm)	α	β	γ	τ
T2A	S690	250×10	150×6	9.6	0.6	12.5	0.6
T2B	S690	250×10	150×6	9.6	0.6	12.5	0.6
T4	S690	250×10	200×6	9.6	0.8	12.5	0.6
T5	S690	250×10	200×10	9.6	0.8	12.5	1.0

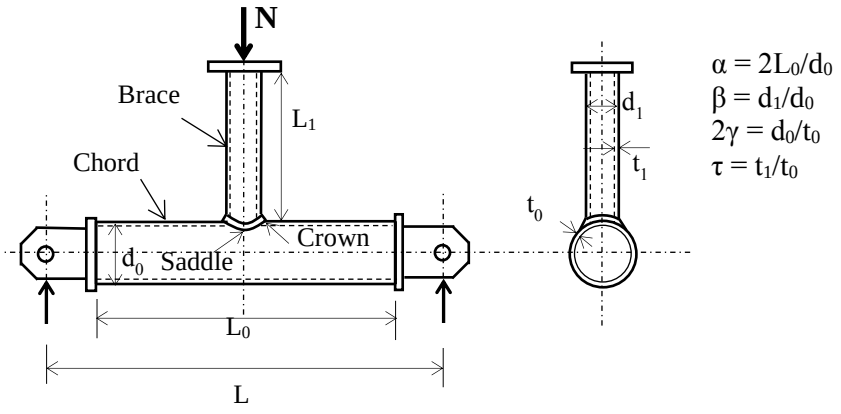

Figure 1. Configuration of a typical T-joint

The following geometrical parameters are covered: i) the brace to chord diameter ratio ($\beta = d_1 / d_0$) is assigned to range from 0.6 to 0.8, ii) the ratio of brace wall thickness to chord wall thickness ($\tau = t_1 / t_0$) is assigned to range from 0.8 to 1.0. The diameter of the chord is assigned

to be 250 mm, and its thickness is 10 mm. The measured geometric dimensions of the four T-joint specimens are summarized in Table 2.

Standard tensile tests were conducted to obtain basic material properties of the S690 steel plates. A summary of key results of the standard tensile tests are shown in Table 3. Edge preparation was performed at the ends of the braces in order to make profiled connecting surfaces for joint welding. The chords and the braces were then connected together through a combination of partial penetration butt welds and fillet welds. Welding of all these T-joints was performed by a highly skilled welder in a well-equipped fabricator. The welding electrode ER110S-G (with a diameter of 1.2 mm) according to AWS A5.28 (AWS 2005) was employed for GMAW of high strength S690 steels. The nominal yield strength of the welding electrode is 720 N/mm^2.

Table 2. Measured geometric dimensions of test specimens

Specimen	Steel grade	Chord length L_0 (mm)	Chord diameter d_0 (mm)	Brace length L_1 (mm)	Brace diameter d_1 (mm)
T2A	S690	1198.8	251.6	599.4	152.6
T2B	S690	1198.8	251.5	599.4	152.0
T4	S690	1199.0	251.8	599.2	200.9
T5	S690	1198.5	251.5	599.4	201.3

Table 3. Material test results of high strength S690 steel

Plate thickness (mm)	Young's modulus E (kN/mm^2)	Yield strength f_y (N/mm^2)	Tensile strength f_u (N/mm^2)	Elongation at fracture ε_f (%)
6	201	745	826	15.9
10	203	787	835	17.8

2.2. Test setup and test procedures

Figure 2 illustrates typical test setup and instrumentation for the joint tests. All these tests were carried out at the Structural Engineering Research Laboratory of the Hong Kong Polytechnic University. Both ends of the chord of each T-joint were attached to two vertical supports through two steel pins. Only in-plane rotations were allowed at both ends of the chord. Two laser levels were installed in front of and at the left of the T-joint during testing to ensure the centre of the brace was carefully aligned with the centre of the loading attachment.

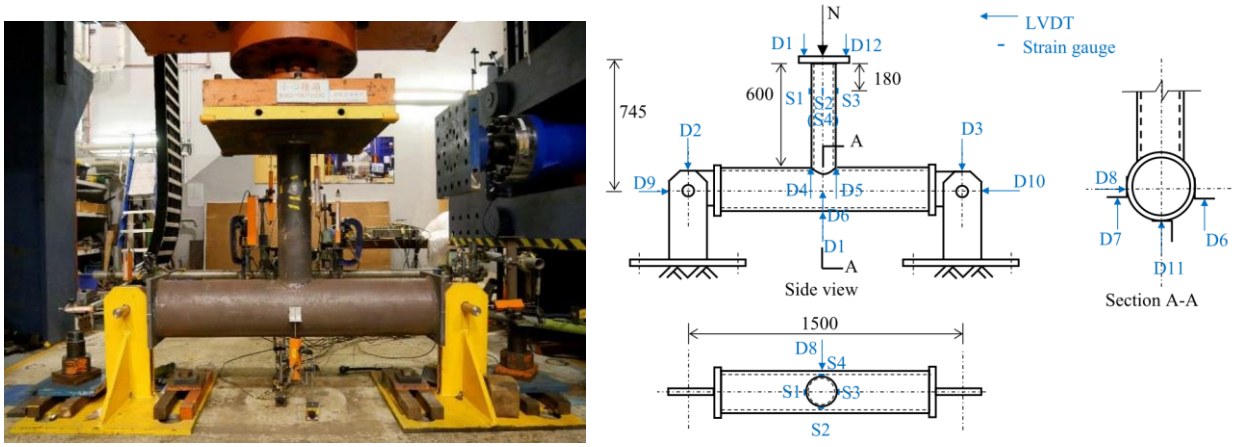

Figure 2. Test setup and instrumentation

2.3. Test results

2.3.1 Failure modes

All the T-joints were tested successfully and they all failed in an interaction between a global failure mode and a local failure mode as follows:

- Overall plastic bending of the chord
- Local plastification of the chord at the joint panel zone

This is because the axial compression force acting on the brace induces a bending moment and a shear force in the chord. The chord section at the joint panel zone is, therefore, under compressive stresses. Such compressive chord stresses will reduce the joint resistance. The deformed shapes and the typical failure mode of these T-joints are illustrated in Figure 3. No weld cracking was observed in all these tests.

Local plastic deformation of the chord

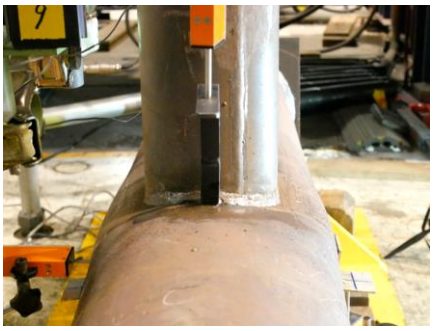

Out-of-plane ovalization of the chord

Figure 3. Typical local failure of Joint T2A

2.3.2 Load-chord indentation curves

The vertical displacement at the mid-span of the chord of each T-joint is calculated as follows

$$\delta = \frac{D_6 + D_7}{2} \tag{1}$$

The maximum indentation, or distortion, is found to occur at the crown point of the chord. Hence, this deformation, namely, chord indentation Δ, is taken as the maximum relative deformation at the crown points and the centre of the chord, which is calculated according to

$$\Delta = \max(D_4 - \delta, D_5 - \delta) \tag{2}$$

The applied load versus chord indentation curve of Joint T2A is shown in Figure 4.

2.3.3 Joint resistances

In the present study, the maximum load resistance of each T-joint is defined by the lower value of: i) the applied ultimate load, and ii) the applied load corresponding to an ultimate deformation limit, where the deformation limit is proposed by Lu et al. (1993). This out-of-plane deformation limit is defined as 3% of the outer diameter of the chord, i.e. $0.03d_0$, according to CIDECT Design Guide 1. It is observed from the applied load versus chord indentation curves that all the tested joints reached the ultimate loads prior to the deformation limit, i.e. $0.03d_0$ or 7.5 mm. Hence, the applied ultimate load of each joint is determined as its axial compressive resistance. The design resistances of all the T-joints are summarized in Table 4. For Joints T4 and T5, the calculated maximum bending moments in the chords all exceed the plastic moment resistances of the chords. Hence, an overall failure mode of chord bending is

considered to be dominant in these joints. However, a local failure mode of chord plastification is considered to be dominant in Joints T2A and T2B through a back analysis on the maximum bending moments in the chords.

By comparing results of Joints T4 and T5, it is shown that the resistance of a T-joint does not always increase by increasing the wall thickness of the brace. Both CIDECT Design Guide 1 and EN1993-1-8 are considered to be structurally adequate for prediction of the axial resistances of these T-joints without the need of applying a reduction factor of 0.9 or 0.8. With these reduction factors, both formulae give an under-prediction of about 25% to 71%. The safety margin is considered to be quite large. Therefore, the strength reduction factor of 0.8 defined by EN 1993-1-12 (CEN 2007) is considered to be very conservative for these T-joints.

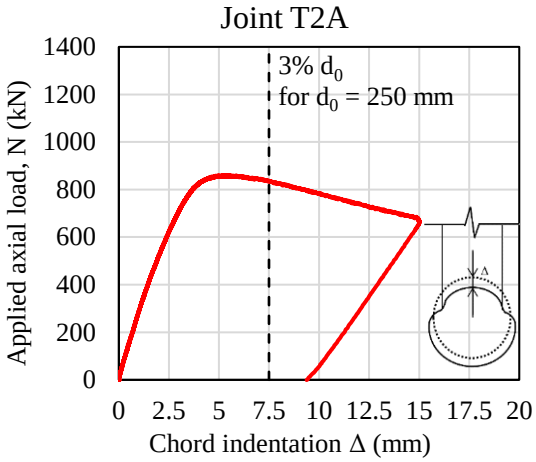

Figure 4. Applied load-chord indentation curve of Joint T2A

Table 4. Summary of test results of T-joints between S690 CFCHS

Joint	$N_{c,Test}$ (kN)	$M_{0,Test}$ (kNm)	$M_{pl,0}$ (kNm)	$M_{0,Test}/M_{pl,0}$	N_{CIDECT} (kN)	$N_{c,Test}/N_{CIDECT}$	N_{EC3} (kN)	$N_{c,Test}/N_{EC3}$	$N_{c,FE}$ (kN)	$N_{c,FE}/N_{c,Test}$
T2A	861	290.6	342.3	0.85	690	1.25	546	1.58	864	1.00
T2B	920	310.5	342.3	0.91	690	1.33	546	1.68	931	1.01
T4	1223	397.5	342.4	1.16	871	1.40	688	1.78	1244	1.02
T5	1175	381.8	342.4	1.12	871	1.35	688	1.71	1248	1.06

Notes: $N_{c,Test}$ denotes the measured strength of T-joints;
$M_{0,Test}$ denotes the calculated maximum bending moment in the chord;
$M_{pl,0}$ denotes the plastic moment resistance of the chord;
N_{CIDECT} denotes the ultimate resistance predicted by CIDECT Design Guide 1; and
N_{EC3} denotes the ultimate strength predicted by according to EN 1993-1-8.

3. NUMERICAL INVESTIGATION

3.1. Proposed finite element model

Nonlinear finite element models of these four T-joints between S690 CFCHS with brace axial compression are established and analyzed using the commercial finite element programme ABAQUS (2009). In the present study, solid elements C3D8R are employed for modeling the T-joints. Three layers of solid elements are employed through the thickness of the CFCHS in order to capture local bending behaviour. A general mesh size of 6mm is determined through a mesh sensitivity study, after considering both computational efficiency and accuracy of the

numerical results. An overall view of the finite element mesh of a typical T-joint is shown in Figure 5. Partial penetration butt-welds are simplified as deep penetration fillet welds in accordance with EN 1993-1-8. The stress-strain curves of the S690 steel plates of 6 and 10 mm thick obtained from standard tensile tests are converted to true stress-strain curves, as illustrated in Figure 6. Stress-strain curves of S690 welds are simplified using an elastic-perfect plastic model. The initial elastic modulus of the weld metal is taken as 210 kN/mm^2, according to EN 1993-1-1 (CEN 2005) while the yield strength of the weld metal is 720 N/mm^2. The Poisson's ratio is taken as 0.3. Isotropic hardening rule and von Mises yield criterion are adopted.

The boundary conditions of the proposed FE models are shown in Figure 7. Three reference points are set, and they are coupled with the nodes on both surfaces of the chord ends and the top surface of the brace with all six degrees of freedom. An axial load is applied onto Reference Point A through the static Riks method given in ABAQUS/Standard.

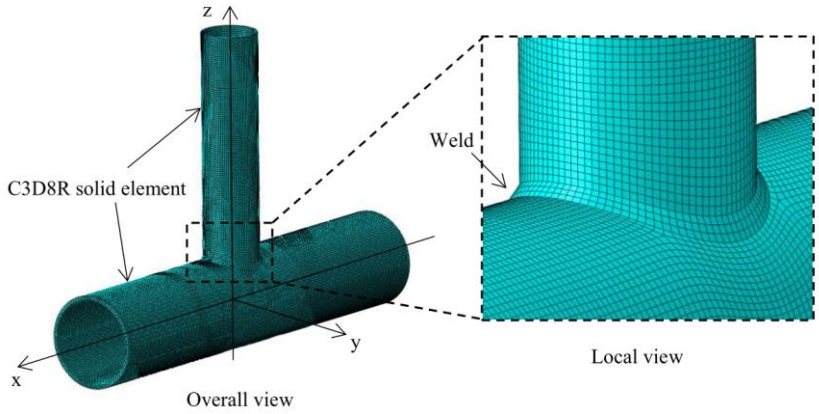

Figure 5. Finite element mesh of a typical T-joint

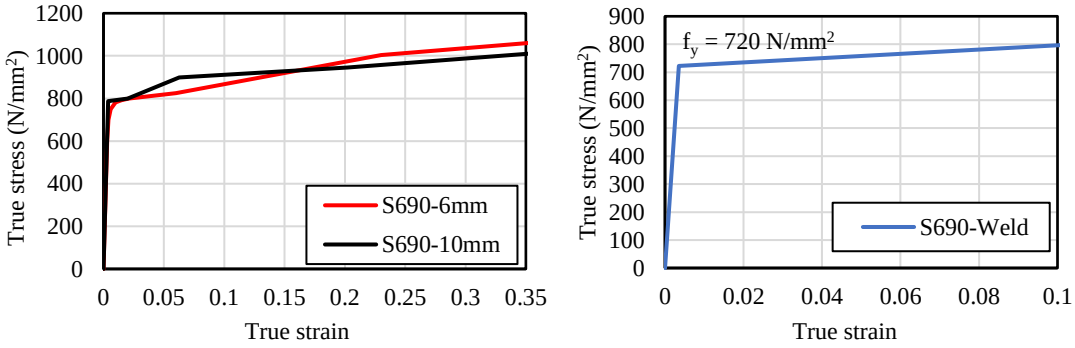

Figure 6. True stress-strain curves for numerical study

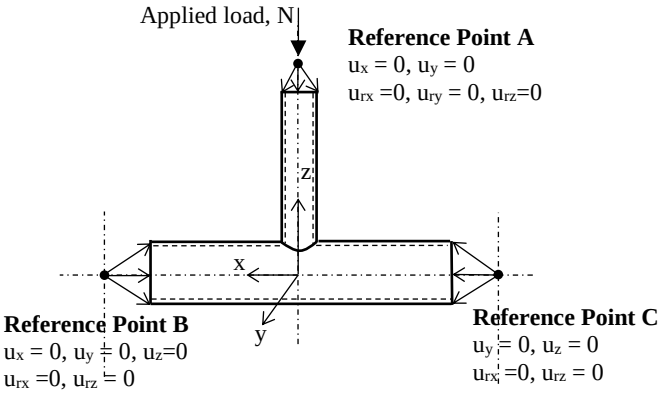

Figure 7. Boundary conditions for the FE models

3.2. Validation of numerical models

Both the measured and the predicted axial load versus chord indentation curves of Joint T2A are compared in Figure 8. Figure 9 illustrates the predicted deformed shapes and stress contours of Joint T2A.The axial resistances from the numerical results are also compared with the test results in Table 3. The differences between the measured and the predicted axial resistances of these T-joints are lower than 6%, with a mean value of the axial resistance ratio $N_{c,FE}$ / $N_{c,Test}$ of 1.02. Therefore, the proposed numerical models are found to be able to predict structural behaviour of these T-joints under brace axial compression well.

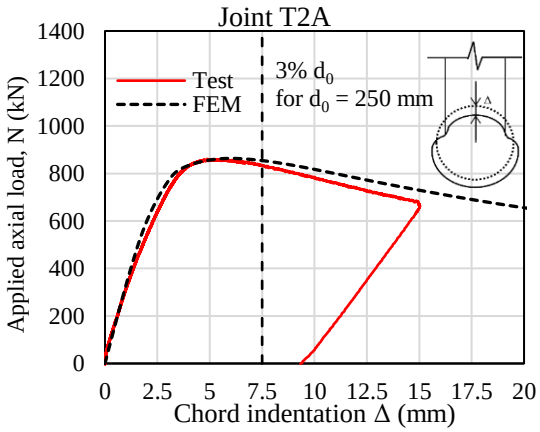

Figure 8. Comparison of load-chord indentation curves of T-joints between CFCHS

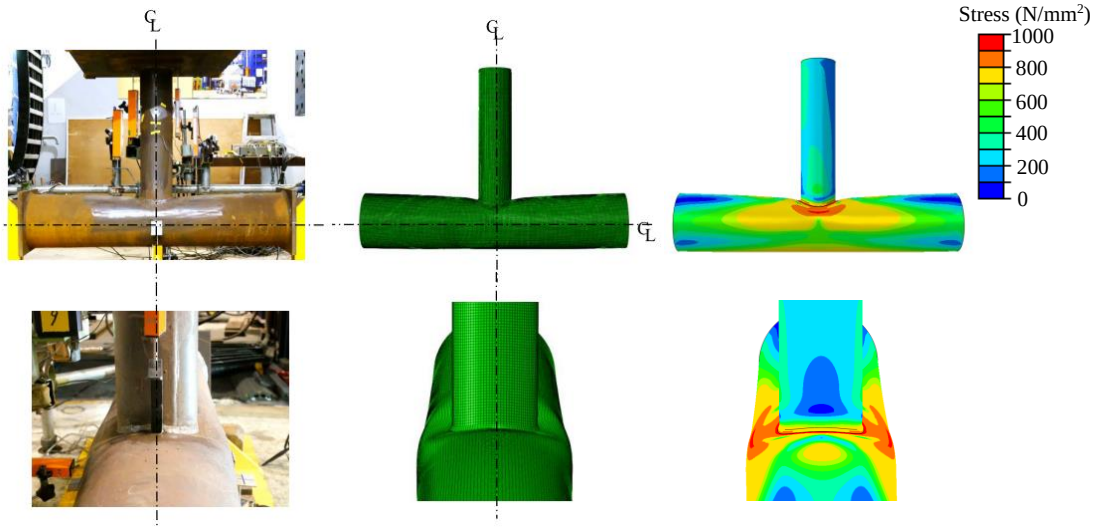

Figure 9. Deformed shapes and stress contours of Joint T2A

4. CONCLUSIONS

In this paper, an experimental and numerical investigation into structural behaviour of T-joints between S690 CFCHS is presented. It should be noted that:

a) A total of four T-joints between S690 CFCHS have been successfully tested under brace axial compression. All test specimens are found to have sufficient strength and ductility.

b) Current design rules provided in CIDECT Design Guide 1 and EN1993-1-8 are considered to be structurally adequate for prediction of the axial resistances of these T-joints between S690 CFCHS with a large safety margin.

c) Three dimensional finite element models have been established and they have been validated to be effective to predict the structural behaviour of T-joints between S690 CFCHS under brace axial compression.

Both the test data of the experimental work and the numerical data to be generated by the calibrated finite element models will facilitate development of efficient design rules for axial compressive resistances of S690 T-joints under brace axial compression.

ACKNOWLEDGEMENTS

The project leading to publication of this paper is partially funded by the Research Grants Committee of the Hong Kong Polytechnic University (Project No. RTZX) and the Research Grants Council of the University Grants Committee of the Government of Hong Kong SAR (Project Nos. PolyU 152194/15E, PolyU 152687/16E and PolyU 152331/17E). The authors also wish to acknowledge the Chinese National Engineering Research Centre for Steel Construction (Hong Kong Branch) at the Hong Kong Polytechnic University for financial support.

REFERENCES

ABAQUS 6.12, (2009), Theory Manual 2009, Providence, US: Dassault Systems Simulia Corp.

AWS, (2005), Specification for Low-Alloy Steel Electrodes and Rods for Gas Shielded Arc Welding, Structural Welding Code – Steel. Miami, United States: American Welding Society.

CEN, (2005), BS EN 1993-1-1, Eurocode 3: Design of steel structures Part 1-1: General rules and rules for buildings, European Committee for Standardization.

CEN, (2005), BS EN 1993-1-8, Eurocode 3: Design of steel structures Part 1-8: Design of joints, European Committee for Standardization.

CEN, (2007), BS EN 1993-1-12, Eurocode 3: Design of steel structures Part 1-12: Additional rules for the extension of EN 1993 up to steel grades S700, European Committee for Standardization.

International Institute of Welding (IIW), (1981), Design recommendations for hollow section joints—predominantly statically loaded, IIW Doc. XV-701-89, 1st edition.

International Institute of Welding (IIW), (1989), Design recommendations for hollow section joints—predominantly statically loaded, IIW Doc. XV-701-89, 2nd edition.

International Institute of Welding (IIW), (2009), Design recommendations for hollow section joints—predominantly statically loaded, IIW Doc. XV-701-89, 3rd edition.

Lu, L. H., De Winkel, G. D., Yu, Y., & Wardenier, J., (1994), Deformation limit for the ultimate strength of hollow section joints. 6th International Symposium on Tubular Structures, 341-347.

Qian, X. D., Choo, Y. S., Van Der Vegte, G. J., & Wardenier, J., (2008), Evaluation of the new IIW CHS strength formulae for thick-walled joints, Proceedings of the 12th International Symposium on Tubular Structures, Shanghai, 271-280.

Wardenier, J., Kurobane, Y., Packer, J. A., Van der Vegte, G. J., & Zhao, X. L., (2008), Design guide for circular hollow section (CHS) joints under predominantly static loading, CIDECT.